Supporting Information

A poorly soluble organic electrode material for high energy density lithium primary batteries based on a multi-electron reduction

Zifeng Chen[a], Pengfei Sun[a], Panxing Bai[a], Hai Su[a], Jixing Yang[a]*, Yang Liu[b]*, Yunhua Xu[a]* and Yanhou Geng[c,d]

Z. F. Chen, P. F. Sun, P. X. Bai, H. Su, Prof. J. X. Yang, Prof. Y. H. Xu
[a]School of Materials Science and Engineering, Key Laboratory of Advanced Ceramics and Machining Technology (Ministry of Education) and Tianjin Key Laboratory of Composite and Functional Materials, Tianjin University, Tianjin 300072, China.
Email: jackieyang@tju.edu.cn, yunhua.xu@tju.edu.cn

Dr. Y. Liu
[b]National Institutes for Food and Drug Control, Beijing 102625, China.
Email: yangliu@nifdc.org.cn

Prof. Y. Geng
[c]School of Materials Science and Engineering and Tianjin Key Laboratory of Molecular Optoelectronic Science, Tianjin University, Tianjin 300072, P. R. China.
[d]Joint School of National University of Singapore and Tianjin University, International Campus of Tianjin University, Binhai New City, Fuzhou 350207, P. R. China.

Experimental Section

Materials: All chemical materials were purchased from commercial sources and used without further purification.

*Synthesis of compound **1***: 2,5-dibromo-*p*-xylene (5.000 g, 19.09 mmol), phenylboronic acid (5.825 g, 47.73 mmol), $Pd(OAc)_2$ (8.5 mg, 0.038 mmol), K_2CO_3 (13.09 g, 94.71 mmol) and tetrabutylammonium bromide (TBAB, 12.22 g, 37.90 mmol) were added to a three-neck round bottom bottle flushed with nitrogen. Then 40 mL nitrogen-bubbled H_2O was injected into the bottle. The mixture was stirred at 70 ºC for two hours and then cooled and extracted with toluene. The product was washed with brine and dried by $MgSO_4$. After evaporation, the residual was recrystallized with ethyl acetate and compound **1** was obtained with a yield of 75%. ^{1}H NMR (400 MHz, $CDCl_3$) δ (ppm) 7.45-7.33 (m, 10H), 7.16 (s, 2H), 2.28 (s, 6H). ^{13}C NMR (100 MHz, $CDCl_3$): δ (ppm) 141.78, 140.90, 132.63, 131.89, 129.25, 128.09, 126.77, 19.73.

*Synthesis of compound **2***: Compound **1** (800 mg, 3.09 mmol) and $KMnO_4$ (2.30 g, 14.6 mmol) were added into 20 mL pyridine and 1.8 mL H_2O and stirred and heated at reflux for two hours. 3 mL H_2O and 1 g $KMnO_4$ were added every half hour for 4 times. After 5 hours, 20 mL H_2O was added and kept at 120 ºC overnight. When cooled down to ambient temperature, the precipitate was filtered and acidized by concentrated hydrochloric acid. The product was collected and dried at 80 ºC overnight in a vacuum oven. Yield: 80%. ^{1}H NMR (400 MHz, DMSO-d_6) δ (ppm) 13.12 (s, 2H), 7.68 (s, 2H), 7.47-7.40 (m, 10H). ^{13}C NMR (100 MHz, $CDCl_3$): δ (ppm) 169.26, 140.02, 134.69, 131.43, 129.40, 128.89, 128.48, 128.09.

Synthesis of IFDO: Compound **2** (700 mg, 2.20 mmol) was added into 35 mL concentrated sulfuric acid and stirred for 2.5 hours. The mixture was then poured onto ice followed by addition of saturated K_2CO_3 solution, and washed for a few hours. Purple precipitate was filtered and washed with water and methanol till the filtrate was colorless. The purple product was dried at 100 ºC in vacuum. Yield: 80% ^{1}H NMR (400 MHz, $CDCl_3$) δ (ppm) 7.82 (s, 2H), 7.70 (d, *J*= 8.0, 2H), 7.57-7.56 (m, 4H), 7.38-7.34 (m, 2H).

Materials characterization: FTIR spectra were recorded by Bruker Alpha P spectrometer with reflection mode in emission from 4000 to 400 cm^{-1}. SEM images were obtained on S4800 SEM (Hitachi, Japan) operated at 5 kV. TGA curve was conducted with Rigaku TG-DTA 8121 in air at a heating rate of 10 ºC min^{-1} from room temperature to 600 ºC. NMR spectra of synthesized compounds and soaked electrodes were obtained from Bruker 400-MHz spectrometer in chloroform-d ($CDCl_3$) or dimethyl sulfoxide-d_6 (C_2D_6SO) at room temperature with tetramethylsilane (TMS) as internal reference. GC-MS measurements were carried out on TRACE 1310/ISQ. XPS measurements were conducted on Thermo Fisher ESCALAB-250Xi+. DFT calculations were carried out with the Gaussian 09 package program by means of B3LYP/6-31+ G(d).

Electrochemical measurements: IFDO electrodes were prepared by mixing IFDO compound, super P and sodium alginate aqueous solution (15 mg mL^{-1}) in a ratio of 6:3:1 (wt%)

to form a slurry that was casted on an aluminum foil by a doctor blade. The electrodes were dried in vacuum at 50 ºC for 12 hours. CR2032 coin-type cells were fabricated in argon-filled glove box (O_2 < 0.1 ppm, H_2O < 0.1 ppm) using lithium metal as counter electrodes, PP separators and electrolyte of 0.5 M $LiClO_4$ in DME or DME with 10% FEC. CV measurements were carried out on Solartron Analytical 1400 (AMETEK, USA) at a scan rate of 0.01 mV s^{-1} between 1.5-3.0 V. The galvanostatic charge/discharge tests were performed on a NEWARE battery test system in a voltage range of 1.5-3.0 V. The galvanostatic discharge profiles were obtained by using constant temperature and humidity test chamber (BHT-80D, Dongguan Bell Experiment Equipment Co., Ltd., China).

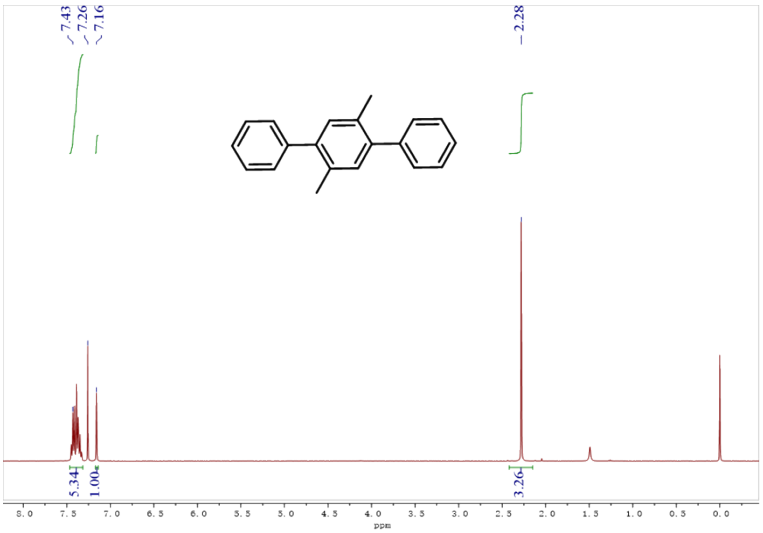

Fig. S1 ^{1}H spectrum of compound **1** in $CDCl_3$.

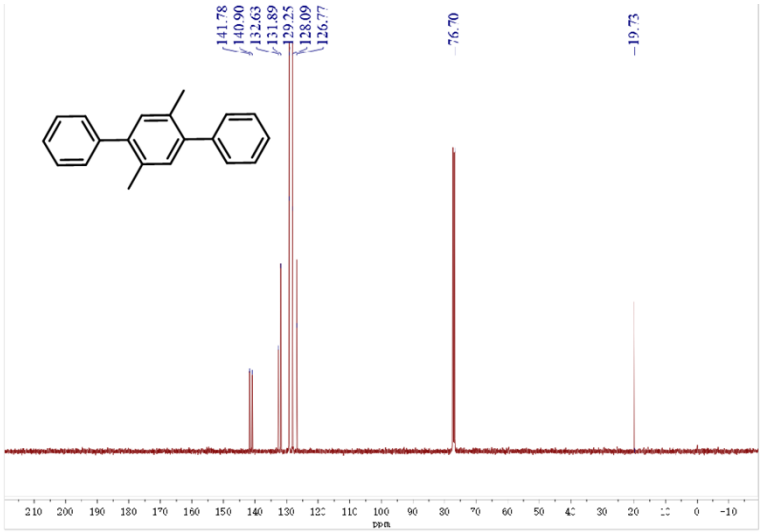

Fig. S2 ^{13}C spectrum of compound **1** in $CDCl_3$.

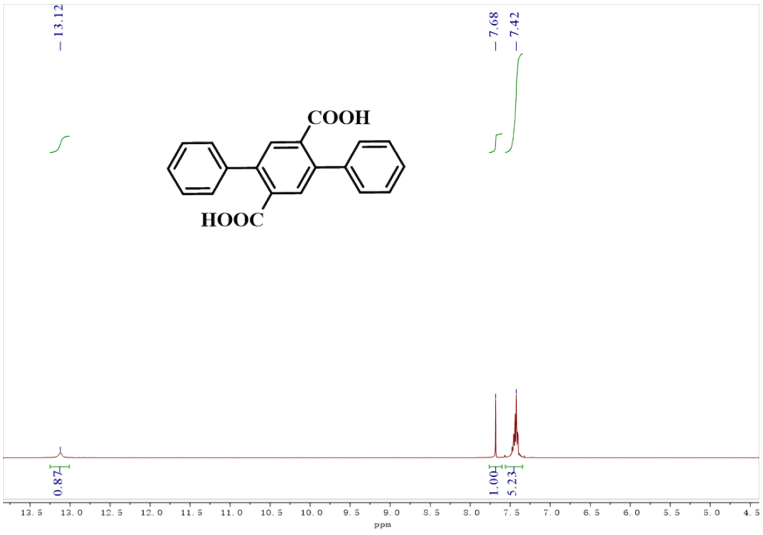

Fig. S3 ^{1}H spectrum of compound **2** in *d*-DMSO.

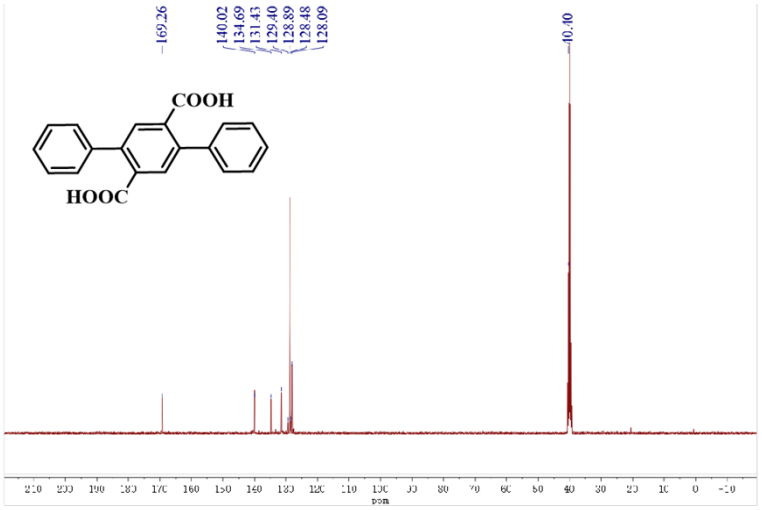

Fig. S4 ^{13}C spectrum of compound **2** in *d*-DMSO.

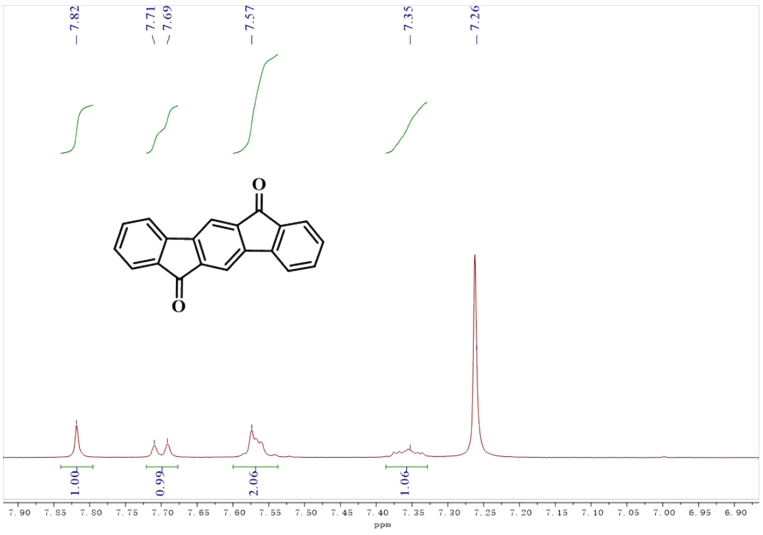

Fig. S5 ^{1}H spectrum of IFDO in $CDCl_3$.

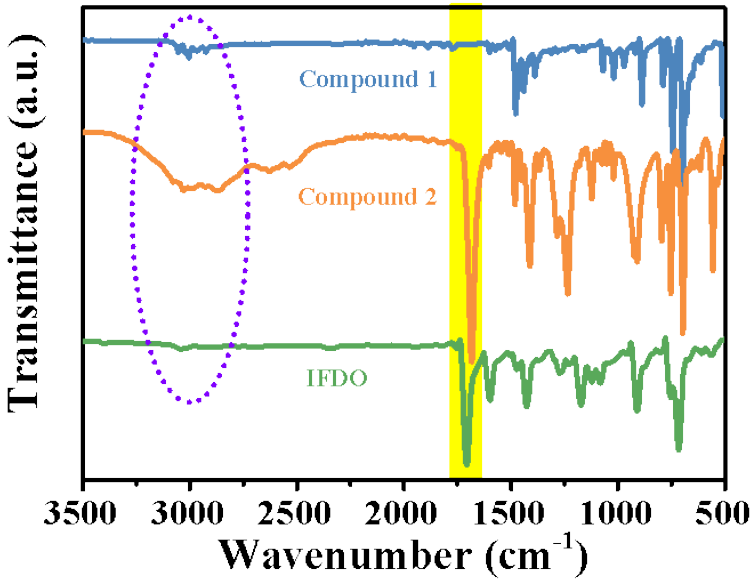

Fig. S6 FTIR spectra of compound **1**, **2** and IFDO.

Compared to Compound **1**, Compound **2** exhibits a broad characteristic vibration peak of -OH in -COOH ranging from 3200-2700 cm^{-1}. Meanwhile, a strong peak centered at 1678 cm^{-1} is attributed to the stretching vibration peak of C=O in -COOH. The results verified that the $-CH_3$ in Compound **1** was successfully oxidized to -COOH. In the spectrum of IFDO, the broad peak ranging from 3200-2700 cm^{-1} vanished and a new peak located at 1709 cm^{-1} appeared, which is attributed to the stretching band of C=O. The results proved the successful synthesis of target compound IFDO.

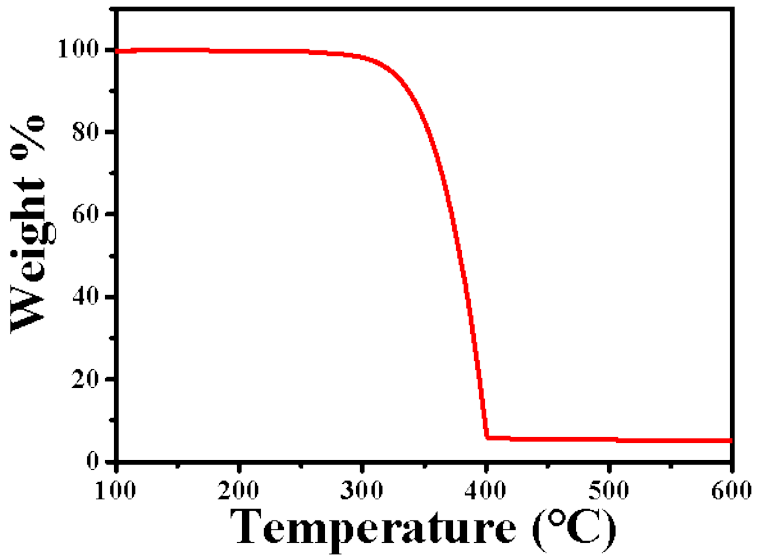

Fig. S7 TGA curve of IFDO in air at a heating rate of 10 ºC min^{-1}.

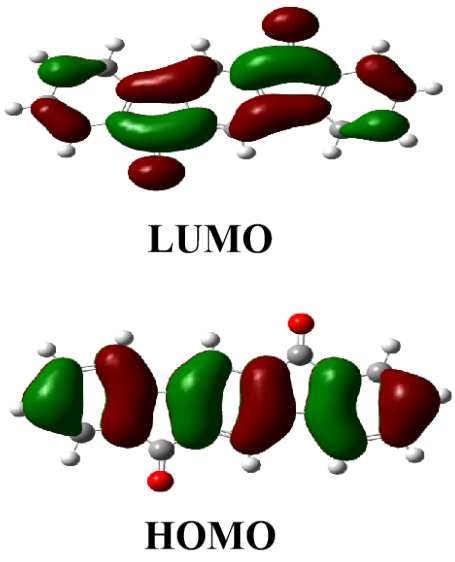

Fig. S8 Frontier molecular orbitals (HOMO and LUMO) of IFDO compounds.

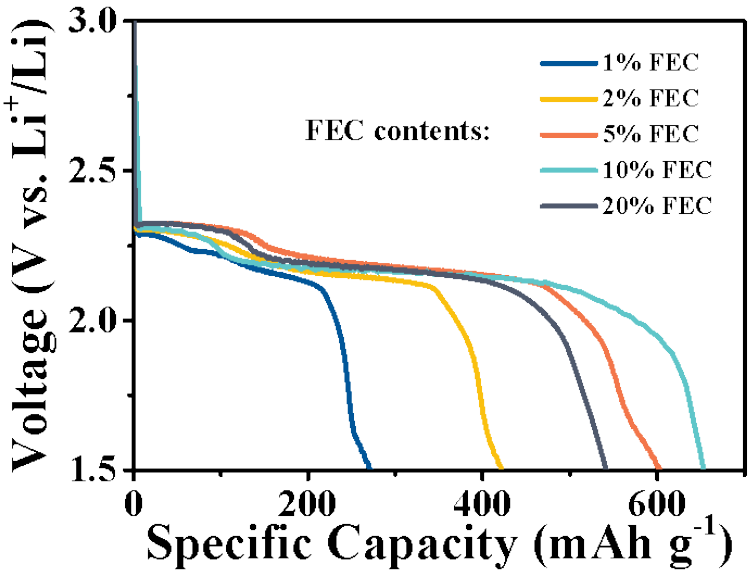

Fig. S9 Galvanostatic discharge profiles of IFDO in the electrolytes with FEC contents ranging from 1% to 20%.

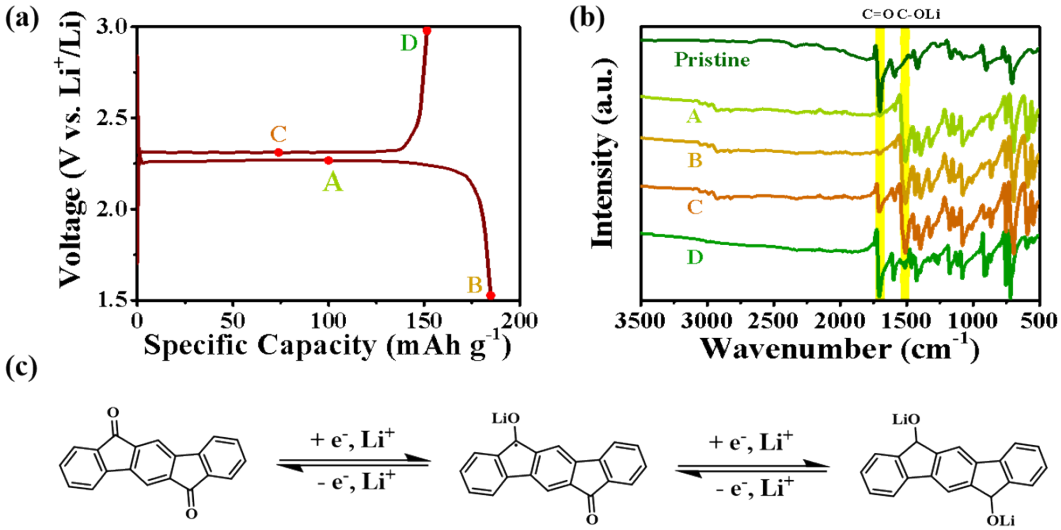

Fig. S10 (a) Galvanostatic charge/discharge profiles of IFDO in FEC-free electrolyte; (b) FTIR spectra of IFDO at different charge/discharge states marked in (a); (c) Redox mechanism of IFDO in the electrolyte of 0.5 M $LiClO_4$ in DME.

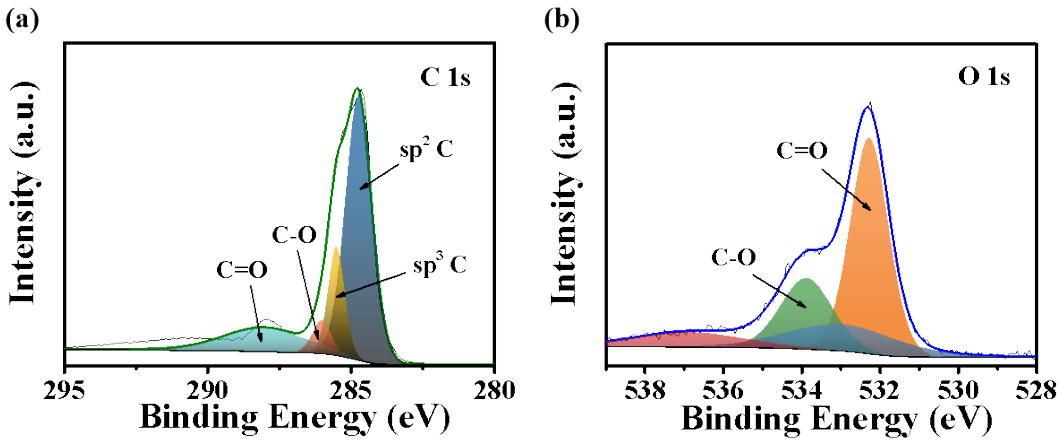

Fig. S11 XPS spectra of (a) C 1s and (b) O 1s of pristine IFDO electrode.

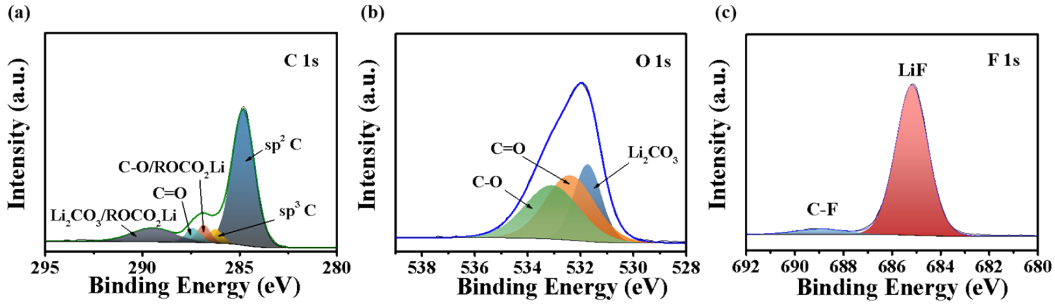

Fig. S12 XPS spectra of (a) C 1s; (b) O 1s and (c) F 1s of IFDO electrode discharged to 2.3 V in FEC-containing electrolyte.

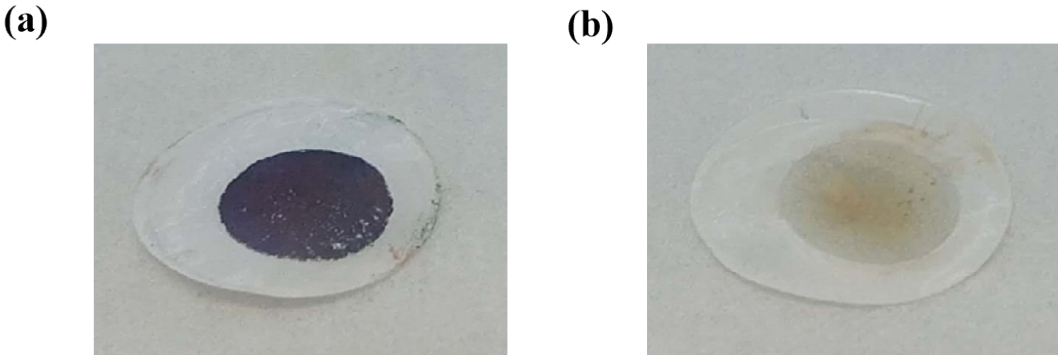

Fig. S13 Digital photographs of separators retrieved at discharged state in the electrolytes (a) without and (b) with FEC.

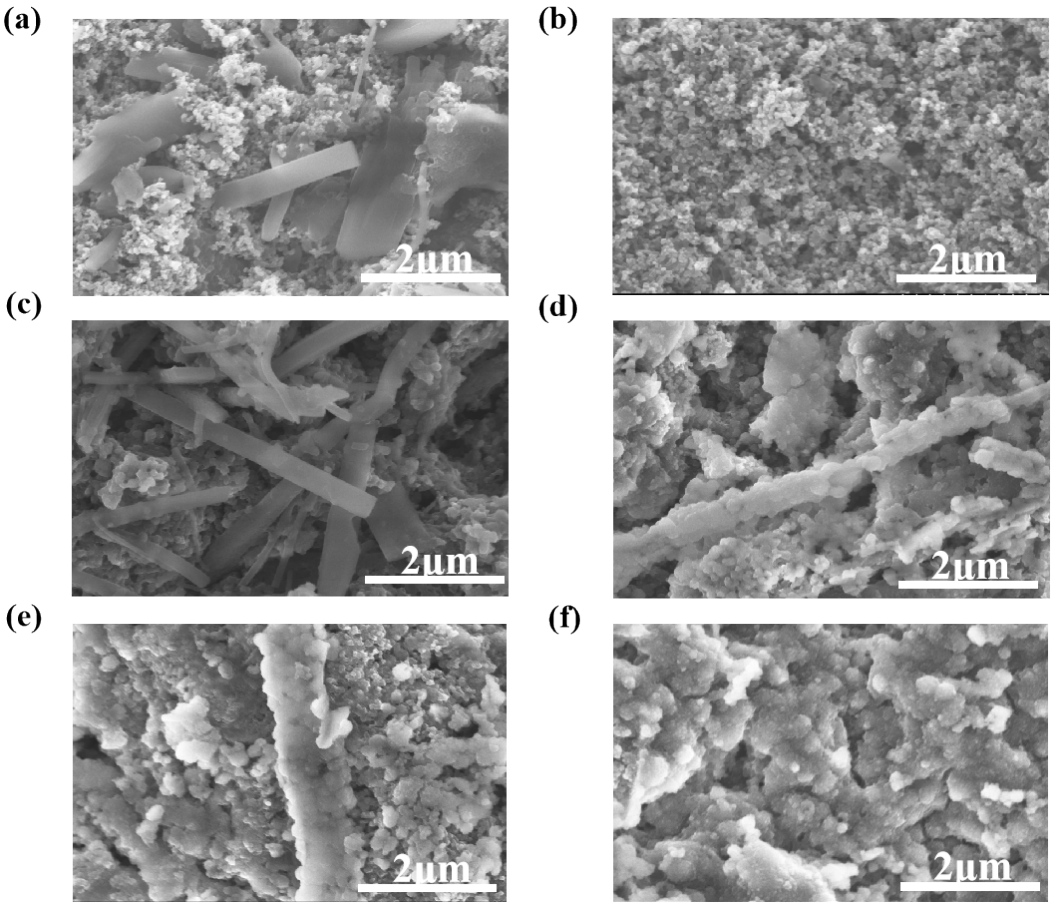

Fig. S14 SEM images of (a) pristine IFDO electrode; (b) discharged electrodes to 1.5 V in FEC-free electrolyte and electrodes discharged to (c) 100 mAh g^{-1}; (d) 300 mAh g^{-1}; (e) 500 mAh g^{-1} and (f) 1.5 V in FEC-containing electrolyte.

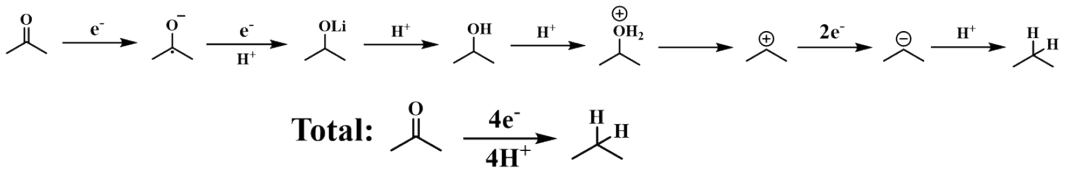

Fig. S15 Proposed reduction mechanism of carbonyl groups to methylene groups.

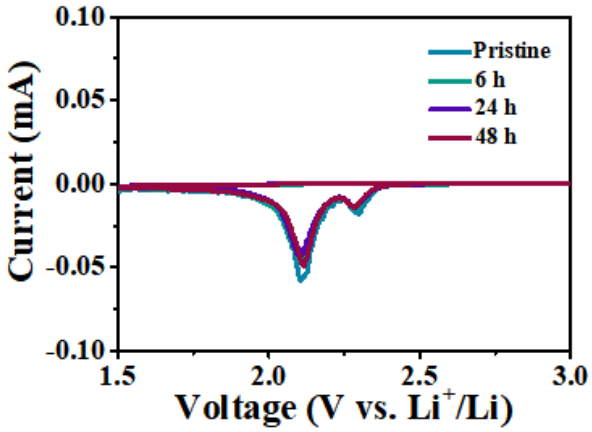

Fig. S16 CV profiles of IFDO in the FEC-containing electrolyte after electrode soaking in DME for different periods of time from 0 to 48 h.

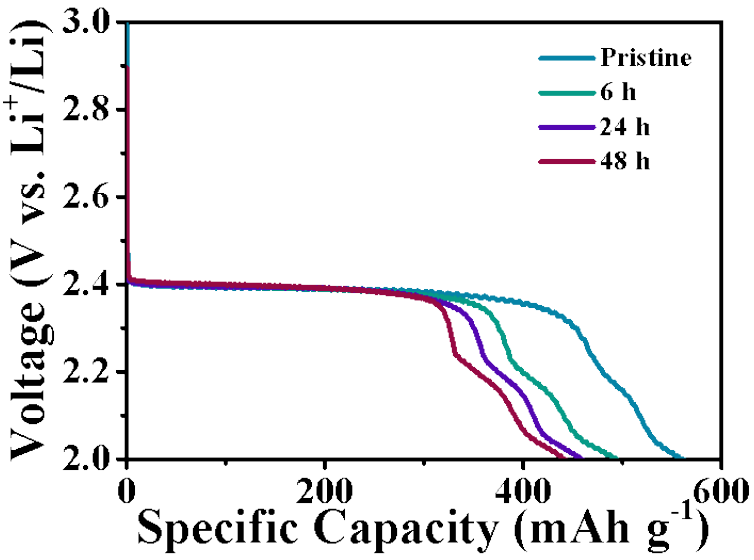

Fig. S17 Galvanostatic discharge profiles of AQ in FEC-containing electrolyte after soaking in DME for different periods.

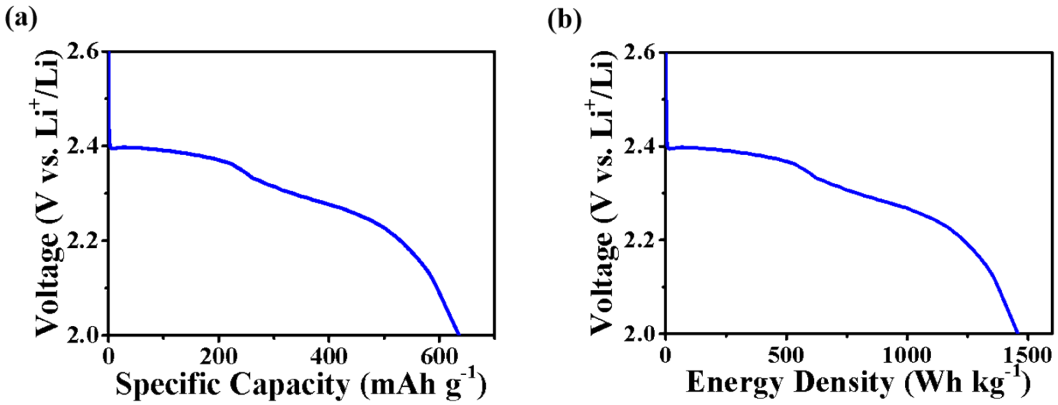

Fig. S18 (a, b) Voltage profiles at 60 ºC.

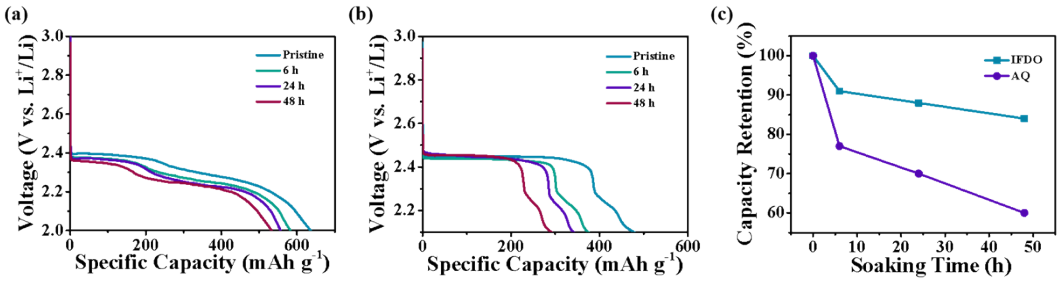

Fig. S19 Galvanostatic discharge curves of (a) IFDO and (b) AQ in FEC-containing electrolyte at 60 ºC after soaking in DMF for different periods; (c) Comparison of capacity retention of IFDO and AQ after soaking different times at 60 ºC.

Table S1 Electrochemical performance comparison of organic cathode materials with high energy densities for LIBs.

Cathode material	Structure	Voltage (V)	Initial discharge capacities (mAh g^{-1})	Energy density (Wh kg^{-1})	Ref
IFDO	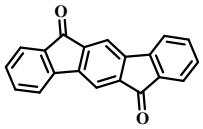 **(poorly soluble)**	**2.13**	**652**	**1392**	**This work**
p-BQ	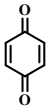 (highly soluble)	2.70	429	1004	1
BBQ	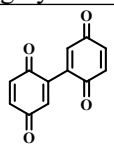 (highly soluble)	2.80	358	917	2
BBQB	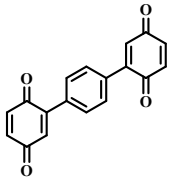 (poorly soluble)	2.60	367	954	3
CF_3-BQ	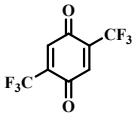 (soluble)	3.00	162	466	4
AQ	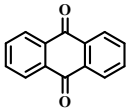 (soluble)	2.40	575	1300	5
BAQB	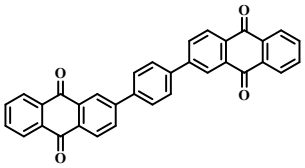 (poorly soluble)	2.18	212	462	6
TBQB	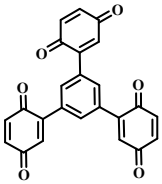 (soluble)	2.60	397	1032	3
$Li_2C_6O_6$	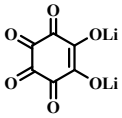 (poorly soluble)	2.10	580	1059	7

PID	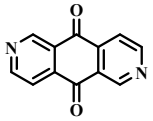 (soluble)	2.71	225	610	8
PhenQ	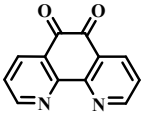 (soluble)	2.74	231	597	9
PTO	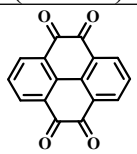 (soluble)	2.59	360	853	9
p-DNB	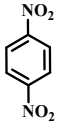 (highly soluble)	2.34	535	1254	10
m-DNB	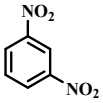 (highly soluble)	2.15	447	963	10
o-DNB	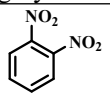 (highly soluble)	2.19	505	1105	10
C4Q	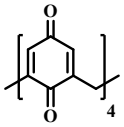 (soluble)	2.60	422	989	11
P5Q	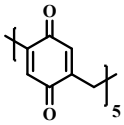 (soluble)	2.60	409	964	12
C_6O_6	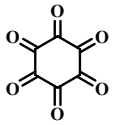 (highly soluble)	1.70	902	1533	13
TCNQ	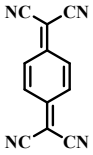 (highly soluble)	2.80	260	682	14
3Q	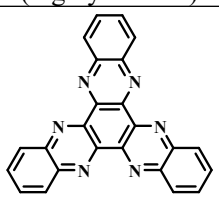 （soluble）	2.00	395	717	15

Li_2-*p*-PDSA	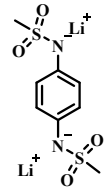 (poorly soluble)	3.77	162	611	16
Li_4-*p*-DHBDS	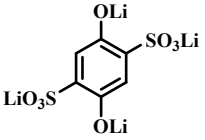 (poorly soluble)	3.35	148	496	17
Li_4-DHPTA	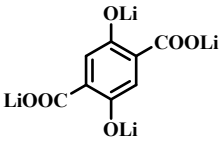 (poorly soluble)	2.60	226	588	18
Li_4-*o*-DHT	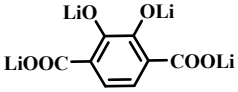 (poorly soluble)	2.85	105	299	19
Lawsone-Li	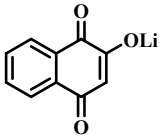 (poorly soluble)	2.37	280	664	20
Et-PXZ	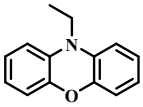 (highly soluble)	3.39	250	845	21
3PXZ	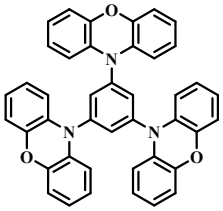 (soluble)	3.70	112	414	22
PBQS	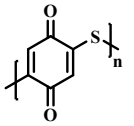	2.67	275	734	1
P14AQ	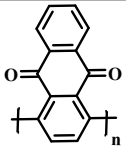	2.14	263	563	23
PBDTD	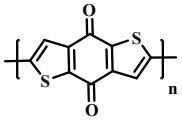	2.50	213	533	24

PTMA	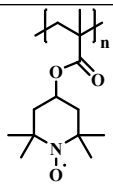	3.55	103	269	25
P-NDI2OD-T2	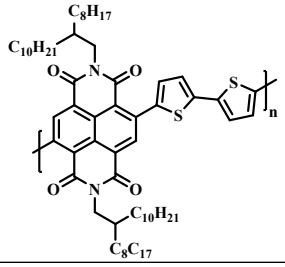	2.40	54	128	26

Table S2 Comparison of solubility and electrochemical performance between IFDO and AQ at room temperature.

Compounds	Solubility in DME (mg mL^{-1})	Solubility in 0.5 M $LiClO_4$ + DME + 10% FEC (mg mL^{-1})	Theoretical Capacity (mAh g^{-1})	Practical Capacity (mAh g^{-1})	Capacity Utilization (%)
IFDO	**0.18**	**0.17**	**760**	**652**	**85.8**
AQ	**3.00**	**2.80**	**1028**	**560**	**54.5**

Table S3 Comparison of solubility and electrochemical performance between IFDO and AQ at an elevated temperature of 60 ºC.

Compounds	Solubility in DME (mg mL^{-1})	Solubility in 0.5 M $LiClO_4$ + DME + 10% FEC (mg mL^{-1})	Theoretical Capacity (mAh g^{-1})	Practical Capacity (mAh g^{-1})	Capacity Utilization (%)
IFDO	**0.75**	**0.80**	**760**	**634**	**83.4**
AQ	**4.80**	**5.00**	**1028**	**476**	**46.3**

References

1. Z. Song, Y. Qian, T. Zhang, M. Otani and H. Zhou, *Adv. Sci.*, 2015, **2**, 1500124.

2. T. Yokoji, Y. Kameyama, N. Maruyama and H. Matsubara, *J. Mater. Chem. A*, 2016, **4**, 5457-5466.

3. J. Yang, P. Xiong, Y. Shi, P. Sun, Z. Wang, Z. Chen and Y. Xu, *Adv. Funct. Mater.*, 2020, **30**, 1959097.

4. T. Yokoji, H. Matsubara and M. Satoh, *J. Mater. Chem. A*, 2014, **2**, 19347-19354.

5. P. Sun, P. Bai, Z. Chen, H. Su, J. Yang, K. Xu and Y. Xu, *Small*, 2020, **16**, 1906462.

6. J. Yang, H. Su, Z. Wang, P. Sun and Y. Xu, *ChemSusChem*, 2020, **13**, 2436-2442.

7. H. Chen, M. Armand, G. Demailly, F. Dolhem, P. Poizot and J. Tarascon, *ChemSusChem*, 2008, **1**, 348-355.

8. Y. Liang, P. Zhang, S. Yang, Z. Tao and J. Chen, *Adv. Energy Mater.*, 2013, **3**, 600-605.

9. Y. Liang, P. Zhang and J. Chen. *Chem. Sci.*, 2013, **4**, 1330-1337.

10. X. Liu and Z. Ye, *Adv. Energy Mater.*, 2020, **11**, 2003281.

11. W. Huang, Z. Zhu, L. Wang, S. Wang, H. Li, Z. Tao, J. Shi, L. Guan and J. Chen, *Angew. Chem., Int. Ed.*, 2013, **52**, 9162-9166.

12. Z. Zhu, M. Hong, D. Guo, J. Shi, Z. Tao and J. Chen, *J. Am. Chem. Soc.*, 2014, **136**, 16461-16464.

13. Y. Lu, X. Hou, L. Miao, L. Li, R. Shi, L. Liu and J. Chen, *Angew. Chem. Int. Edit.*, 2019, **58**, 7020-7024.

14. Y. Hanyu and I. Honma. *Sci. Rep.*, 2012, **2**, 453-458.

15. C. Peng, G. Ning, J. Su, G. Zhong, W. Tang, B. Tian, C. Su, D. Yu, L. Zu, J. Yang, M. Ng, Y. Hu, Y. Yang, M. Armand and K. Loh, *Nat. Energy*, 2017, **2**, 17074-17082.

16. J. Wang, A. Lakraychi, X. Liu, L. Sieuw, C. Morari, P. Poizot and A. Vlad, *Nat. Mater.*, 2021, **20**, 665-673.

17. A. Lakraychi, E. Deunf, K. Fahsi, P. Jimenez, J.-P. Bonnet, F. Djedaini-Pilard, M. Bècuwe, P. Poizot and F. Dolhem, *J. Mater. Chem. A*, 2018, **6**, 19182-19189.

18. S. Wang, L. Wang, K. Zhang, Z. Zhu, Z. Tao and J. Chen, *Nano Lett.*, 2013, **13**, 4404-4409.

19. S. Gottis, A. Barrès, F. Dolhem and P. Poizot, *ACS Appl. Mater. Interfaces*, 2014, **6**,

10870-10876.

20. J. Lee, M and J. Park, *Adv. Energy Mater.*, 2017, **7**, 1602279.

21. S. Lee, K. Lee, K. Ku, J. Hong, S. Park, J. Kwon and K. Kang, *Adv. Energy Mater.*, 2020, **10**, 2001635.

22. K. Lee, I. Serdiuk, G. Kwon, D. Min, K. Kang, S. Park and J. Kwon, *Energy Environ. Sci.*, 2020, **13**, 4142-4156.

23. Z. Song, Y. Qian, M. L. Gordin, D. Tang, T. Xu, M. Otani, H. Zhan, H. Zhou and D. Wang, *Angew. Chem., Int. Ed.*, 2015, **54**, 13947-13951.

24. Y. Jing, Y. Liang, S. Gheytani and Y. Yao, *Nano Energy*, 2017, **37**, 46-52.

25. L. Bugnon, C. J. H. Morton, P. Novak, J. Vetter and P. Nesvadba, *Chem. Mater.*, 2007, **19**, 2910-2914.

26. Y. Liang, Z. Chen, Y. Jing, Y. Rong, A. Facchetti and Y. Yao. *J. Am. Chem. Soc.*, 2015, **137**, 4956-4959.